

Decomposition kinetics of peroxynitrite: influence of pH and buffer

Cite this: *Dalton Trans.*, 2013, **42**, 9898

Christian Molina, Reinhard Kissner and Willem H. Koppenol*

Received 9th April 2013,
Accepted 3rd May 2013

DOI: 10.1039/c3dt50945a

www.rsc.org/dalton

Introduction

Peroxynitrite† is formed from the reaction of NO^\cdot with O_2^\cdot ,³ which proceeds at a diffusion-controlled rate, $k = 1.6 \times 10^{10} \text{ M}^{-1} \text{ s}^{-1}$.^{4,5} Because both NO^\cdot and O_2^\cdot are released by activated macrophages and neutrophils,^{6–11} peroxynitrite can be formed *in vivo*.¹² Due to its oxidizing power and nitrating activity, peroxynitrite is cytotoxic and is associated with inflammatory diseases.¹³

ONOO^\cdot is stable in a cold alkaline solution in the absence of carbonyl compounds and metals. The pK_a of ONOOH increases from 6.5 to 7.3 with increasing phosphate concentration.¹⁴ Isomerization of ONOOH to HNO_3 ,^{15,16} reaction 1,‡ is first-order in ONOOH . Rate constants for the isomerization, obtained over a period of *ca.* 40 years, have slightly decreased, from 1.5 to 1.1 s^{-1} , most likely because of purer preparations of peroxynitrite (Table 1). ONOOH is a powerful one-electron

Institute of Inorganic Chemistry, Department of Chemistry and Applied Biosciences, ETH Zurich, 8093 Zurich, Switzerland. E-mail: koppenol@inorg.chem.ethz.ch

†“Peroxynitrite” refers to a mixture of ONOO^\cdot and ONOOH , depending on the pH; “peroxynitrate” refers to a mixture of $\text{O}_2\text{NOO}^\cdot$ and O_2NOOH , depending on the pH. Buffers: Tris, tris(hydroxymethyl)aminomethane; Hepes, 2-[4-(2-hydroxyethyl)piperazin-1-yl]ethanesulfonic acid; Pipes, 1,4-piperazinediethanesulfonic acid. Formulae, trivial names and systematic names: ONOO^\cdot , peroxynitrite, (dioxido)oxidonitrate(1–); ONOOH , peroxynitrous acid, (hydridodioxido)oxidonitrogen; $\text{O}_2\text{NOO}^\cdot$, peroxynitrate, (dioxido)dioxidonitrate(1–); O_2NOOH , peroxynitric acid, (hydridodioxido)dioxidonitrogen; NO^\cdot , nitric oxide, oxidonitrogen(·) or nitrogen monoxide; O_2^\cdot , superoxide, dioxide(·[–]) or dioxidanidyl; HNO_3 , nitric acid, hydroxidodioxidonitrogen; HO^\cdot , hydroxyl, hydridooxygen(·) or oxidanyl; NO_2^\cdot , pernitric oxide, nitrogen dioxide or dioxidonitrogen(·); CO_2 , carbon dioxide, dioxidoxygen; CO_3^{2-} , trioxido-carbonate(·[–]); CO_3^{2-} , carbonate, trioxido-carbonate(2–); HCO_3^- , hydrogencarbonate, hydridooxidodioxido-carbonate(1–); NO_2^- , nitrite, dioxidonitrate(1–); O_2 , dioxygen; H_2O_2 , hydrogen peroxide or dioxidane.^{1,2}

‡Reactions 1–5 are part of Scheme 1.

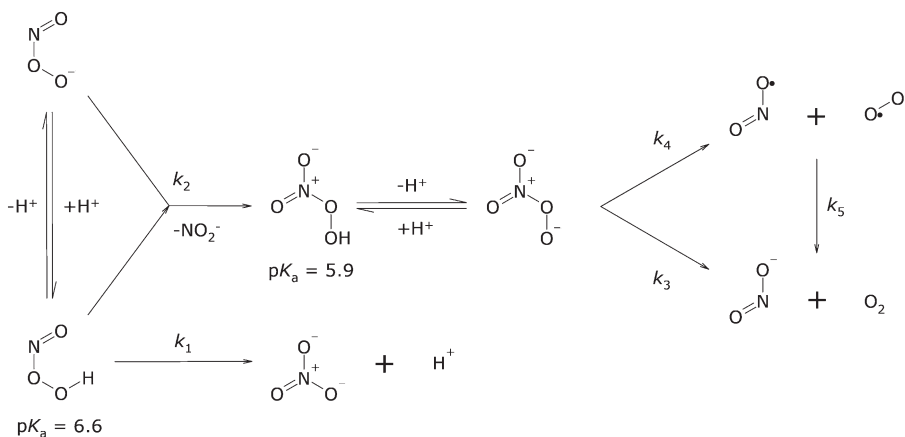
Table 1 The literature values for rate constant k_1 of the isomerization of ONOOH at 25 °C

Year	Reference	k_1/s^{-1}	Remarks
1970	28	1.5	<i>a,b</i>
1990	12	0.65 ± 0.05	<i>a,c</i>
1992	17	1.3	<i>a</i>
1993	29	1.0 ± 0.2	<i>a</i>
1997	30	1.25	<i>a</i>
1997	14	1.20	$I = 0.2 \text{ M}$
1998	31	1.20	$I = 0.1 \text{ M}$
2003	32	1.10 ± 0.05	$I = 0.9 \text{ M}$
2012	This work	1.11 ± 0.01	$I = 0.2 \text{ M}$

^a Ionic strength is not given. ^b At r.t. ^c At 37 °C.

and two-electron oxidant.^{17,18} A review of the literature shows that evidence for the much-cited homolysis of ONOOH to HO^\cdot and NO_2^\cdot is weak: at most 5% of ONOOH may undergo this reaction.¹⁹ In any case, the reaction of otherwise stable ONOO^\cdot with CO_2^{20} is far more relevant to biology ($k = (3–5.8) \times 10^4 \text{ M}^{-1} \text{ s}^{-1}$)^{21,22} as it yields, in part, very oxidising species, NO_2^\cdot and CO_3^{2-} with $E^\circ(\text{NO}_2^\cdot/\text{NO}_2^-) = 1.04 \text{ V}^{23}$ and $E^\circ(\text{CO}_3^{2-}/\text{CO}_3^{2-}) = 1.59 \text{ V}^{24}$. These species are responsible for the higher yield of nitration of phenols compared to nitration by peroxynitrite alone (4–9% without and 14–19% with 20 mM HCO_3^-).^{22,25–27}

Deviations from first-order behaviour³³ and formation of O_2^{34} and NO_2^\cdot in a 1:2 stoichiometric ratio³⁵ have been observed. Both phenomena can be explained with an additional reaction, namely between ONOOH and ONOO^\cdot , a disproportionation that, given a pK_a of ONOOH of nearly 7, is only relevant near and above neutral pH (Scheme 1). This disproportionation thus fits the observation that NO_2^\cdot yields increase with pH and with peroxynitrite concentration.^{36,37} Gupta *et al.*³⁸ showed that the disproportionation reaction



Scheme 1

yields initially O₂NOO⁻ and NO₂⁻. O₂NOOH has a pK_a of 5.9^{39,40} and is relatively stable. When one compares the wavelengths of maximal absorptivity and the extinction coefficients of ONOO⁻ and O₂NOO⁻, one sees that these parameters are quite similar: O₂NOO⁻ absorbs with $\epsilon_{\text{max}} = 1650 \text{ M}^{-1} \text{ cm}^{-1}$ at 285 nm,³⁹ and ONOO⁻ with $\epsilon_{\text{max}} = 1705 \text{ M}^{-1} \text{ cm}^{-1}$ at 302 nm.⁴¹ Furthermore, the rates of decay of both ONOOH and O₂NOO⁻ are close to 1 s⁻¹ (see below). For these reasons O₂NOO⁻ went unnoticed as an intermediate during the decay of peroxy nitrite. The decomposition of O₂NOO⁻ yields NO₂⁻ and O₂,³⁹ of which ca. 1–2% is in an excited (¹Δ_g O₂) state.⁴² Estimates for decomposition reaction 3 at 25 °C are $k_3 = 1.0 \pm 0.2 \text{ s}^{-1}$,³⁹ $1.35 \pm 0.03 \text{ s}^{-1}$,⁴³ and 0.58 s^{-1} .³⁸ k_4 and k_{-4} are estimated to be $1.05 \pm 0.23 \text{ s}^{-1}$ ⁴³ and $(4.5 \pm 1.0) \times 10^9 \text{ M}^{-1} \text{ s}^{-1}$,³⁹ respectively. Redox reaction 5 is thermodynamically favoured, $\Delta_{\text{rxn}5} G^\circ = -118 \text{ kJ mol}^{-1}$. $\Delta_f G^\circ (\text{kJ mol}^{-1})$ values in aqueous solution are 62.5 for NO₂,⁴⁴ 33.8 for O₂⁻,⁴⁵ –38 for NO₂⁻,^{23,44} and 16.4 for O₂,⁴⁶ the reaction proceeds with $k_5 = 1 \times 10^8 \text{ M}^{-1} \text{ s}^{-1}$.⁴⁷ We emphasise that the formation of O₂NOO⁻, a reaction that is second-order in peroxy nitrite, is biologically insignificant, because the concentration of peroxy nitrite that may be generated by activated macrophages is very low. However, upon bolus additions of peroxy nitrite during *in vitro* experiments that result in initial concentrations exceeding 0.1 mM, the formation of peroxy nitrate should be taken into account.

In neutral 0.1 M tris(hydroxymethyl)aminomethane (Tris) buffer, decomposition of peroxy nitrite yields up to 40% peroxy nitrate with $k_2 = 3 \times 10^4 \text{ M}^{-1} \text{ s}^{-1}$.³⁸ Decomposition of peroxy nitrite in various neutral amine buffers, *e.g.* 2-[4-(2-hydroxyethyl)-piperazin-1-yl]ethanesulfonic acid (HEPES) or 1,4-piperazine-diethanesulfonic acid (PIPES), yields an oxidant that was suggested to be H₂O₂.⁴⁸ However, it could well have been O₂NOOH. The pH of peroxy nitrite containing samples is usually controlled by phosphate buffer, and rarely by Tris or HEPES buffer (*e.g.* ref. 49 and 50). At equal pH, similar initial peroxy nitrite concentrations yield more NO₂⁻ in Tris buffer⁵⁰ than in phosphate buffer.³⁶ This indicates that a Tris-dependent conversion of peroxy nitrite to NO₂⁻ takes place. The possibility that the buffer influences the course or result of a

reaction has rarely been considered.^{48,51} We therefore also compared decomposition kinetics of peroxy nitrite at pH = 6.8 in buffers that contain variable concentrations of phosphate and Tris and refined the decomposition model by taking into account reactions (1)–(3).

Materials and methods

Materials

(Me₄N)OONO was prepared according to the work by Bohle *et al.*,⁵² dissolved in 0.01 M NaOH and frozen as 25 mM solutions. NaH₂PO₄·H₂O (s), Na₂HPO₄·12H₂O (s), H₂NC(CH₂OH)₃ (s), NaOH (s), 85% H₃PO₄ (aq), and 70% HClO₄ (aq), all of analytical grade, were purchased from Sigma-Aldrich/Fluka (Buchs, CH), Brenntag Schweizerhall AG (Basel, CH), Merck (Darmstadt, DE), Riedel-de Haen (Seelze, DE) and used as received. Ar and N₂, both of 99.995% purity, were taken from the in-house gas supply. All solutions were prepared in deionized water that was further purified by using a Milli-Q unit from Millipore AG (Zug, CH).

Preparation of solutions

All solutions were prepared, stored, transferred and mixed at room temperature in glass vessels under Ar or N₂ and used within one day. Because ONOO⁻ is sensitive to acid, heat and light, samples (1.4 g) of deeply frozen 25 mM (Me₄N)OONO (aq) were dissolved in ice-cold 20 mM aqueous NaOH to produce alkaline ONOO⁻ solutions that were stored and transferred at 0 °C and kept in the dark. The fresh alkaline ONOO⁻ solutions contained ONOO⁻, NO₂⁻ and NO₃⁻ in a molar ratio of 10:1:1 (see the section ‘Determination of peroxy nitrite, nitrite and nitrate’). The impurity by NO₂⁻ and NO₃⁻ in the alkaline ONOO⁻ solutions is most probably formed during the thawing of frozen (Me₄N)OONO (aq).⁵³ Because the pK_a of ONOOH depends on the ionic strength of the medium,¹⁴ the ionic strength of the Tris buffers and the pH-varied 0.07 M phosphate buffers was adjusted to 0.2 M by the addition of NaClO₄, which we assume to be inert. Considering the

ion-pairing of Na^+ with HPO_4^{2-} ⁵⁴ we calculated the ionic strength of our samples at pH 6–8 to be between 0.197 M and 0.206 M. The $\text{p}K_a$ of ONOOH is 6.7 under these conditions.

Determination of peroxynitrite, nitrite and nitrate

The content of peroxynitrite and of its typical ionic decomposition products – NO_2^- and NO_3^- – were quantified for the lot of deeply frozen (Me_4N)OONO (aq) used for kinetics experiments as described before.³⁶ Briefly, a sample (1.4 g) of deeply frozen (Me_4N)OONO (aq) was subsequently weighted, dissolved in ice-cold 2 mM NaOH and analysed by spectrophotometry at 302 nm (Specord 250 from Analytik Jena AG, Jena, DE). To determine the content of NO_2^- and NO_3^- , a sample (1.4 g) of deeply frozen (Me_4N)OONO (aq) was dissolved in 30 ml ice-cold 2 mM NaOH. 1 ml of this alkaline solution was added to 5 ml ice-cold 2 mM phosphoric acid to yield a mixture with pH = 3. In an acidic solution, peroxynitrite is mainly present as ONOOH, which isomerises to NO_3^- . This acidic solution was neutralised after 5 min by the addition of 4 ml 2 mM NaOH and then analysed by ion chromatography (Super Sep IC Anion Column from Metrohm AG, Herisau, CH) with a phthalate eluent of pH = 4.7 and by conductometric detection (732 IC Detektor from Metrohm AG, Herisau, CH). To determine the content of NO_3^- in the (Me_4N)OONO (aq) sample, the peroxynitrite content was subtracted from the content of NO_3^- , which resulted after isomerization of ONOOH. The amount of peroxynitrate was not determined because it decays very fast in an alkaline medium.

Stopped-flow experiments

The decay of peroxynitrite was initiated by a rapid 1 : 1 mixing of an alkaline ONOO^- solution with an acidic buffer solution in a thermostated (25 °C) stopped-flow unit (SX17MN) from Applied Photophysics (Leatherhead, UK) and observed for 10 s by spectrophotometry. Monochromatic light at the absorption maximum of ONOO^- , 302 nm, was used.

For each sample the decay of the absorption was measured at least four times, and the decay traces were averaged before analysis. The initial absorption of each mixture was used to calculate $[\text{ONOO}^-]_0$: the optical path length is 1 cm, and $\epsilon_{302\text{ nm}}(\text{ONOO}^-) = 1705\text{ M}^{-1}\text{ cm}^{-1}$.⁴¹

Prior to each decay experiment, the total initial peroxynitrite concentration in the sample, $[\text{ONOO}^-]_{0,\text{total}}$, was derived from the absorbance of a 1 : 1 mixture of an alkaline ONOO^- solution with 20 mM NaOH. Then the experiments were carried out at the desired pH in a specific buffer. Prior to switching to another pH and buffer, the standardization with NaOH was repeated. For each mixture, the final pH value was measured by an Orion Microprocessor Ionalyzer 901 from Thermo Scientific after mixing, outside the stopped-flow apparatus. For the decay simulations, the $\text{p}K_a$ of ONOOH was calculated from the measured pH, $[\text{ONOO}^-]_0$ and $[\text{ONOO}^-]_{0,\text{total}}$ at pH = 6.8.

Computations

We assume that at pH < 6 ONOOH isomerises to NO_3^- and H^+ exclusively; the decay of ONOOH was fitted to a single exponential function that resulted in k_{obs} . The rate constant k_1 was derived from k_{obs} , which is a function of pH, $\text{p}K_a(\text{ONOOH})$ and k_1 :

$$k_{\text{obs}} = k_1 \frac{[\text{H}^+]}{[\text{H}^+] + K_a(\text{ONOOH})} \rightarrow k_1 = k_{\text{obs}} \left(1 + \frac{K_a(\text{ONOOH})}{[\text{H}^+]} \right) \quad (1)$$

Reactions (1)–(3)§ lead to rate laws 2 and 3 for peroxynitrite and peroxynitrate.

$$\frac{\partial[\text{ONOO}^-]_{\text{total}}}{\partial t} = -k_1[\text{ONOOH}] - 2k_2[\text{ONOOH}][\text{ONOO}^-] \quad (2)$$

$$\frac{\partial[\text{O}_2\text{NOO}^-]_{\text{total}}}{\partial t} = k_2[\text{ONOOH}][\text{ONOO}^-] - k_3[\text{O}_2\text{NOO}^-] \quad (3)$$

Given the $\text{p}K_a$ values of ONOOH and O_2NOO , we calculated the time-dependent concentrations of the absorbing species ONOO^- and O_2NOO^- .

$$\frac{\partial[\text{ONOO}^-]}{\partial t} = -k_1 \frac{[\text{H}^+][\text{ONOO}^-]}{[\text{H}^+] + K_a(\text{ONOOH})} - 2k_2 \frac{[\text{H}^+][\text{ONOO}^-]^2}{[\text{H}^+] + K_a(\text{ONOOH})} \quad (4)$$

$$\frac{\partial[\text{O}_2\text{NOO}^-]}{\partial t} = k_2 \frac{K_a(\text{O}_2\text{NOO})[\text{H}^+][\text{ONOO}^-]^2}{([\text{H}^+] + K_a(\text{O}_2\text{NOO}))([\text{H}^+] + K_a(\text{ONOOH}))} - k_3 \frac{K_a(\text{O}_2\text{NOO})[\text{O}_2\text{NOO}^-]}{[\text{H}^+] + K_a(\text{O}_2\text{NOO})} \quad (5)$$

With the extinction coefficients $[\epsilon_{302\text{ nm}}(\text{ONOO}^-) = 1705\text{ M}^{-1}\text{ cm}^{-1}; \epsilon_{302\text{ nm}}(\text{O}_2\text{NOO}^-) = 1370\text{ M}^{-1}\text{ cm}^{-1}$ from the spectrum in ref. 38], we reproduced the absorption trace of peroxynitrite solutions at 302 nm. The calculated absorbance trace was fitted to the measured absorbance trace by the variation of the rate constants according to the method of the least squares. All data analysis and model calculations were carried out in Microsoft Excel by macro programmes (which are available from the authors upon request). The kinetics of the mixed-order decomposition of peroxynitrite was quantitatively compared by the use of the first half-life of the absorbance.

Results

Computation of the decomposition rate constants of peroxynitrite in phosphate buffer

From the measurement of the initial absorbance at various pH values, we derive a $\text{p}K_a(\text{ONOOH})$ of 6.7 at $I = 0.2\text{ M}$ which fits with the dependence of the $\text{p}K_a$ on ionic strength.

A rate constant $k_1 = 1.11 \pm 0.01\text{ s}^{-1}$ ($n = 7$, 95% confidence level) was determined by fitting absorbance traces at pH = 5.3 and $I = 0.2\text{ M}$ in 70 mM phosphate buffer (see Fig. 1). At this pH, $[\text{ONOO}^-]$ is too low to contribute to significant

§ Reactions 1–5 are part of Scheme 1 with correspondingly numbered rate constants.

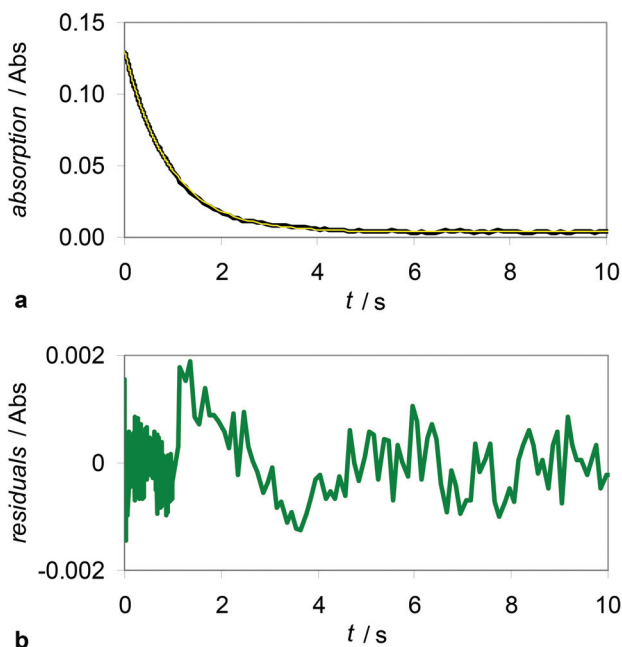


Fig. 1 Decomposition of 0.25 mM peroxynitrite at 25 °C and pH = 5.3 in 0.07 M phosphate buffer ($I = 0.2$ M) and simulation according to isomerization only with $k_1 = 1.11\text{ s}^{-1}$. (a) Actual decay curve measured (black) and simulated (yellow); (b) residuals (green) of the model.

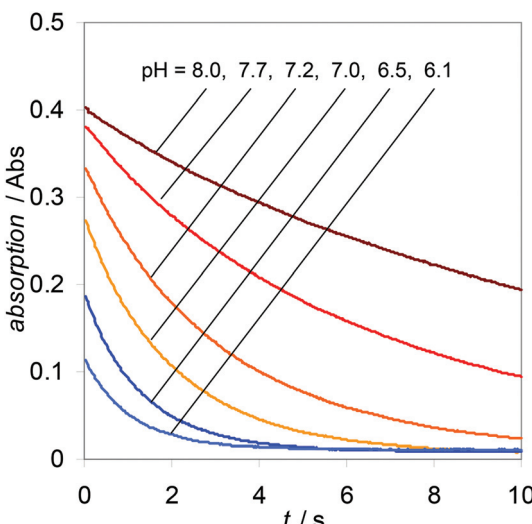


Fig. 2 Four to six decay traces per pH value (0.25 mM peroxynitrite in 70 mM phosphate buffer at 25 °C and $I = 0.2$ M, see Table 2) were measured at 302 nm and averaged.

disproportionation, and $[\text{HNO}_2]$, from the nitrite present in the $(\text{Me}_4\text{N})\text{OONO}$ preparation, is too low to cause undesired reactions.

It became clear that the results obtained at higher pH (Fig. 2) could not be fitted with $k_1 = 1.11\text{ s}^{-1}$ (Fig. 3). We therefore take into account an additional process, disproportionation of peroxynitrite to O_2NOO^- and NO_2^- .³⁸ For the decay of O_2NOO^- to NO_2^- and O_2 , we take a value of 1.35 s^{-1} .⁴³ The

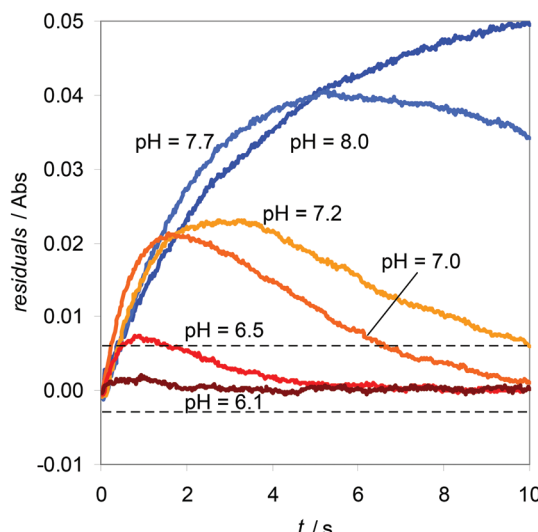


Fig. 3 Four to six decay traces per pH value (0.25 mM peroxynitrite in 70 mM phosphate buffer at 25 °C and $I = 0.2$ M, see Table 2) were averaged and fitted with $k_1 = 1.11\text{ s}^{-1}$. The residuals are much larger than in Fig. 4, the range of which is indicated by the two dashed lines.

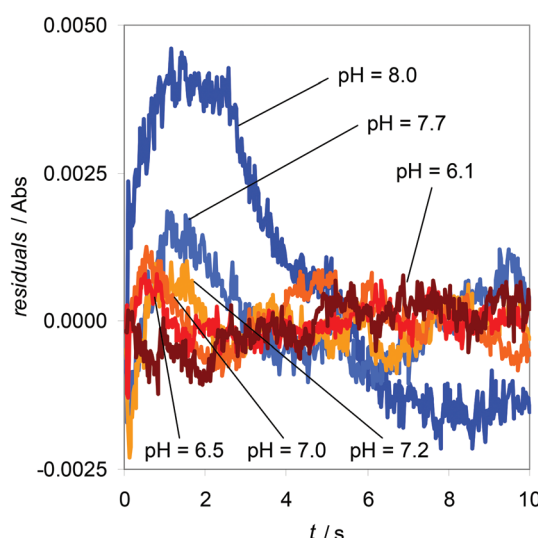


Fig. 4 The same as Fig. 3, but fitted with $k_1 = 1.11\text{ s}^{-1}$ and $k_3 = 1.35\text{ s}^{-1}$.⁴³ k_2 was varied to minimise the residuals shown here.

combination of these three processes allows us to fit the obtained results with significantly smaller errors (Fig. 4).

Fig. 5 shows an actual decay curve of 0.25 mM peroxynitrite at pH = 6.5 which was fitted according to rate laws 2 and 3 with $k_1 = 1.11\text{ s}^{-1}$ and $k_3 = 1.35\text{ s}^{-1}$.⁴³ In addition, the fit required that k_2 be $1163\text{ M}^{-1}\text{ s}^{-1}$: the residuals are very small and do not show any systematic error. This procedure was repeated at various other pH values, and the results for k_2 are presented in Table 2.

The first half-life of the absorbance increases with pH (Fig. 6) because ONOO^- is stable and the isomerization of ONOOH is the predominant decomposition pathway of

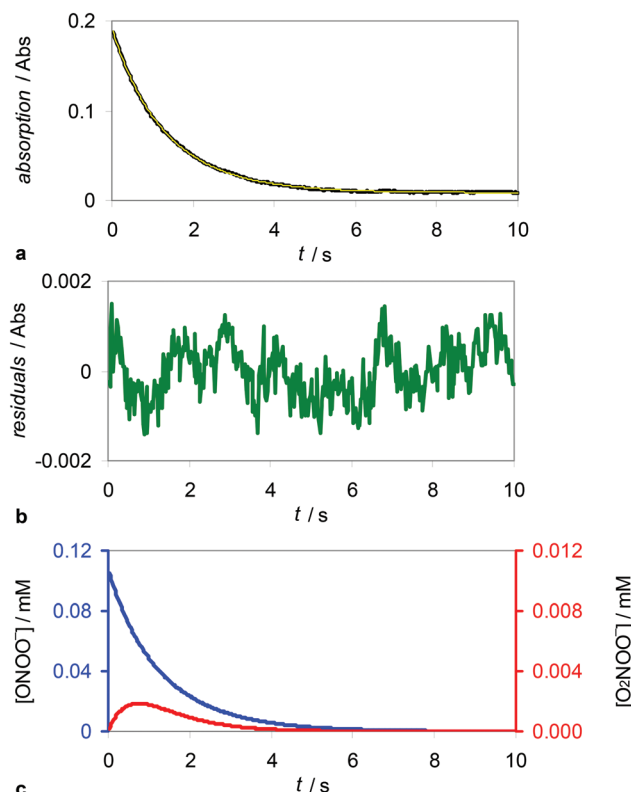


Fig. 5 Decomposition of 0.25 mM peroxynitrite at 25 °C and pH = 6.5 in 0.07 M phosphate buffer ($I = 0.2$ M) and simulation according to rate laws 2 and 3 with $k_1 = 1.11\text{ s}^{-1}$ and $k_3 = 1.35\text{ s}^{-1}$ ⁴³ resulting in $k_2 = 1163\text{ M}^{-1}\text{ s}^{-1}$. (a) Actual decay curve measured (black) and simulated (yellow); (b) residuals (green) of the model; (c) concentrations calculated for ONOO⁻ (blue) and O₂NOO⁻ (red), [ONO₂H] is not shown.

Table 2 Decomposition of 0.25 mM ONOO⁻ at 25 °C in 0.07 M phosphate buffer, $I = 0.2$ M adjusted by NaClO₄, $k_1 = 1.11 \pm 0.01\text{ s}^{-1}$, $k_3 = 1.35\text{ s}^{-1}$ ⁴³ n measurements. The error of 1 is based on all 27 measurements from pH 6.1 to 8.0 at the 95% confidence level

pH	First $t_{1/2}/\text{s}$	$k_2/(10^3\text{ M}^{-1}\text{ s}^{-1})$	n
5.3	0.69 ± 0.01	—	7
6.1	0.76 ± 0.04	0.9 ± 1.0	4
6.5	0.92 ± 0.03	1.3 ± 0.3	4
7.0	1.41 ± 0.02	1.7 ± 0.1	4
7.2	2.21 ± 0.06	1.1 ± 0.1	6
7.7	4.6 ± 0.1	1.4 ± 0.1	5
8.0	9.4 ± 0.1	1.7 ± 0.1	4
Over all pH values		1.3 ± 0.1	27

peroxynitrite. The first half-life of the absorbance at pH 6–8 can be calculated according to rate laws 2 and 3 with $k_1 = 1.11\text{ s}^{-1}$, $k_2 = 1.3 \times 10^3\text{ M}^{-1}\text{ s}^{-1}$ and $k_3 = 1.35\text{ s}^{-1}$ much more accurately than by a model based on a first-order decay only.

Decomposition of peroxynitrite in phosphate buffer and Tris buffer

The decomposition of peroxynitrite is decelerated by phosphate and accelerated by Tris: $t_{1/2} = 0.75\text{--}0.88\text{ s}$ in 0.1 M phosphate and 0.1 M Tris, $t_{1/2} = 1.33\text{--}1.42\text{ s}$ in 0.1 M phosphate

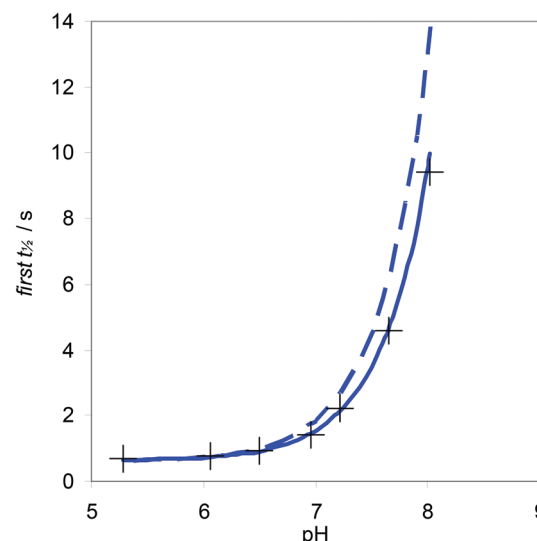


Fig. 6 Decomposition of 0.25 mM peroxynitrite at pH = 5.3, 6.1, 6.5, 7.0, 7.2, 7.7 and 8.05 in 70 mM phosphate buffer ($I = 0.2$ M). The first half-life of the absorbance measured (+) and calculated (blue lines) based on the best fit of two decomposition models: (1) (dashed line) according to isomerization only with $k_1 = 1.11\text{ s}^{-1}$; (2) (solid line) according to rate laws 2 and 3 with $k_1 = 1.11\text{ s}^{-1}$, $k_2 = 1.3 \times 10^3\text{ M}^{-1}\text{ s}^{-1}$ and $k_3 = 1.35\text{ s}^{-1}$.

Table 3 Decomposition of 0.25 mM peroxynitrite at 25 °C and pH = 6.8 in 0.1 M Tris buffers ($I = 0.2$ M) at various phosphate concentrations. n, the number of determinations

[Phosphate]/M	First $t_{1/2}/\text{s}$	$k_2/(10^3\text{ M}^{-1}\text{ s}^{-1})$	n
0	0.65 ± 0.00	14 ± 2	2
0.001	0.68 ± 0.02	13 ± 1	5
0.005	0.69 ± 0.09	13 ± 4	3
0.025	0.73 ± 0.04	12 ± 3	3
0.1	0.91 ± 0.02	9.3 ± 0.4	6

Table 4 Decomposition of 0.25 mM peroxynitrite at 25 °C and pH = 6.8 in 0.1 M phosphate buffers ($I = 0.2$ M) at various Tris concentrations

[Tris]/M	$k_2^a/(10^3\text{ M}^{-1}\text{ s}^{-1})$	$k_2^b/(10^3\text{ M}^{-1}\text{ s}^{-1})$
0	1.3	1.2
1×10^{-4}	^c	1.3
3×10^{-4}	1.3	1.5
1×10^{-3}	1.5	2.0
3×10^{-3}	2.4	2.8
0.01	3.7	4.4
0.03	5.1	5.2
0.1	8.0	9.4

Initial total peroxynitrite concentration: ^a 260 μM and ^b 340 μM. ^c Not determined.

only and $t_{1/2} = 0.63\text{ s}$ in 0.1 M Tris only (Tables 3 and 4, and Fig. 7).

Interestingly, up to a certain concentration, Tris shows no significant influence on the decay of peroxynitrite. However, this concentration decreases with increasing initial peroxynitrite concentration. We find that the measured first half-life

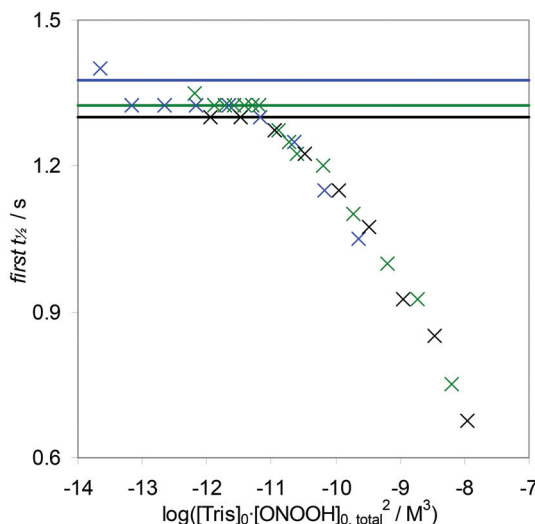


Fig. 7 Decomposition of 0.047 mM (blue), 0.25 mM (green) and 0.34 mM (black) peroxy nitrite at pH = 6.8 in 0.1 M phosphate buffers with varied Tris concentrations. The solid horizontal lines indicate the first half-life of the absorbance of peroxy nitrite in the absence of Tris. When $[Tris]_0 \cdot [ONOO^-]_{0, total}^2$ exceeds $6.3 \times 10^{-12} M^3$, Tris significantly catalyses the disproportionation.

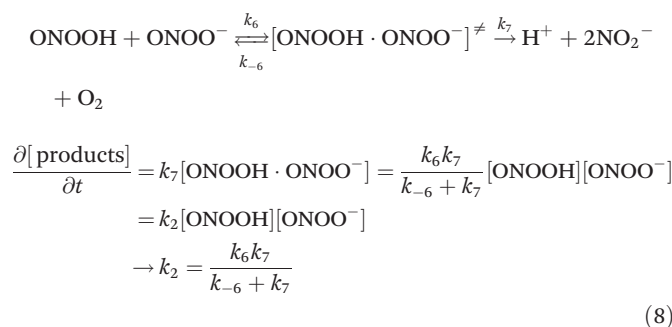
of the absorbance of peroxy nitrite correlates with $[Tris]_0 \cdot [ONOO^-]_{0, total}^2$: if $[Tris]_0 \cdot [ONOO^-]_{0, total}^2$ exceeds $6.3 \times 10^{-12} M^3$ ($1 \times 10^{-11.2} M^3$), then Tris significantly accelerates the decomposition of peroxy nitrite (Fig. 7).

Discussion

According to rate laws 2 and 3, absorption traces are fitted (e.g. Fig. 5) and values of the first half-life of the absorbance are simulated (Fig. 6) without a systematic error for the pH range 6–8. A model restricted to homolysis³⁷ does not simulate the decay of peroxy nitrite in this pH range very well.

The first-order rate constant of the isomerization agrees with earlier results.

The disproportionation can be regarded as a two-step reaction: a reversible association and a subsequent irreversible conversion to the products:



Earlier estimates of the parameters of this sequence are listed in Table 5. The first two are in good agreement with the disproportionation rate constant determined here; however, the third estimate is higher.

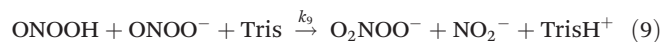
Table 5 Rate constants of the decomposition of peroxy nitrite into NO_2^- and O_2

$k_6/(M^{-1} s^{-1})$	$k_{-6}/(s^{-1})$	$k_7/(s^{-1})$	$k_2/(M^{-1} s^{-1})$	Source
			0.20 ± 0.01	$(2.0 \pm 0.1) \times 10^3$ Decay modelling ¹⁴
2.5×10^5	25	0.2–0.3	$(2\text{--}3) \times 10^3$	Decay modelling ³⁶
1.7×10^4	0.025	0.05	1.1×10^4	Decay modelling ⁵⁵
			$(1.3 \pm 0.1) \times 10^3$	This work

According to rate laws 2 and 3, the concentration of peroxy nitrate reaches its concentration maximum *ca.* 1 s after the decay of peroxy nitrite is initiated (Fig. 5c). After that peak concentration, the second-order disproportionation becomes negligible in comparison with first-order decay processes 1 and 3. Therefore, decay traces of peroxy nitrite deviate from first-order kinetics in the first 1–2 s.³³

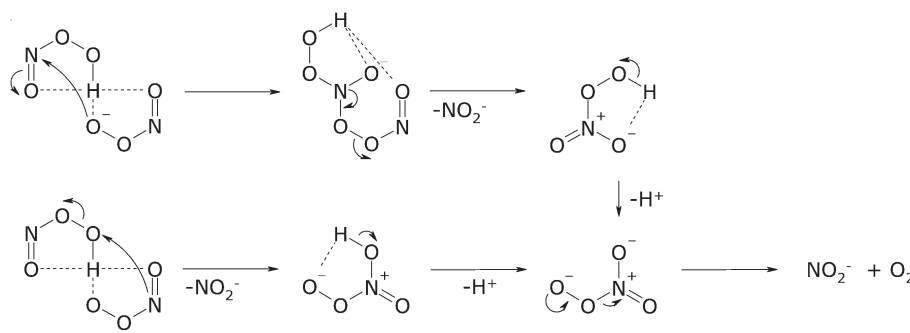
The decomposition model according to reactions (1)–(3)§ and (9) fails to reproduce the Tris-dependent first half-life of the absorbance. It fits the absorption curves with a residual that indicates a systematic error that increases with the Tris concentration (not shown). Moreover, it results in k_2 values that increase non-linearly with the Tris concentration if the latter is higher than $10^{-4} M$ (Table 4). Saturation may cause a non-linear dependence. The accelerating effect of Tris will be addressed in a future publication.

We find that k_2 is one order of magnitude lower in phosphate buffer (this work: $1.3 \times 10^3 M^{-1} s^{-1}$) than in Tris buffer (this work: $9 \times 10^3 M^{-1} s^{-1}$, Gupta *et al.*:³⁸ $3 \times 10^4 M^{-1} s^{-1}$, both in 0.1 M Tris) and that 0.25 mM peroxy nitrite decomposes in 0.1 M Tris buffer twice as fast as it does in 0.1 M phosphate buffer. Therefore, Tris accelerates the disproportionation of peroxy nitrite and thereby increases k_2 . Indeed, the peroxy nitrate yield is, being dependent on the square of the initial peroxy nitrite concentration, 40 times higher in Tris buffer than it is in phosphate buffer.³⁸ The observed rate of decay of peroxy nitrite accelerates with increasing Tris concentration (Fig. 7). Furthermore, the first half-life of the absorbance correlates with the concentration product $[Tris]_0 \cdot [ONOO^-]_{0, total}^2$. The concentration product $[Tris] \cdot [ONOO^-]_{total}^2$ is likely part of the rate law of the additional Tris-dependent decomposition pathway. If the Tris concentration is high enough, this additional decomposition pathway contributes significantly to the overall decomposition. If Tris participates in the disproportionation according to reaction (9) and if k_2 , in Tris = $k_2 + k_9 \cdot [Tris]$, then we obtain an estimate of $k_9 = (8\text{--}29) \times 10^3 M^{-2} s^{-1}$:



It is likely that a more accurate decomposition model can be achieved by considering a chain of association equilibria that involve peroxy nitrite and Tris.

Peroxy acids, in general, decompose in reactions that are first-order in both the acid and its conjugate base: typically with rate constants of $1 \times 10^{-3}\text{--}1 \times 10^{-1} M^{-1} s^{-1}$.^{56–59} These rate constants are much smaller than those found for



Scheme 2

peroxynitrite (1.3×10^3 – 3×10^4 M $^{-1}$ s $^{-1}$). However, in contrast to other peroxyacids, the atom attached to the OOH group of peroxy nitrite has a lone pair that allows additional reactions – electrophilic attack and oxidative addition – that may allow faster decomposition (Scheme 2).

At peroxy nitrite concentrations $>10^{-4}$ M, but at lower concentration in the presence of Tris, disproportionation of peroxy nitrite in samples competes with reactions of peroxy nitrite with target molecules and produces peroxy nitrate that is an artificial reactive intermediate.

Acknowledgements

We thank the SNF and the ETH Zurich for financial support.

References

- 1 N. G. Connelly, T. Damhus, R. M. Hartshorn and A. T. Hutton, *Nomenclature of Inorganic Chemistry. IUPAC Recommendations 2005*, 2005.
- 2 W. H. Koppenol, *Pure Appl. Chem.*, 2000, **72**, 437–446.
- 3 N. V. Blough and O. C. Zafiriou, *Inorg. Chem.*, 1985, **24**, 3502–3504.
- 4 T. Nauser and W. H. Koppenol, *J. Phys. Chem. A*, 2002, **106**, 4084–4086.
- 5 H. Botti, M. Möller, D. Steinmann, T. Nauser, W. H. Koppenol, A. Denicola and R. Radi, *J. Phys. Chem. B*, 2010, **114**, 16584–16593.
- 6 S. Moncada, M. W. Radomski and R. M. J. Palmer, *Biochem. Pharmacol.*, 1988, **37**, 2495–2501.
- 7 J. B. Hibbs, R. R. Taintor, Z. Vavrin and E. M. Rachlin, *Biochem. Biophys. Res. Commun.*, 1988, **157**, 87–94.
- 8 M. R. Green, H. A. O. Hill, M. J. Okolow-Zubkowska and A. W. Segal, *FEBS Lett.*, 1979, **100**, 23–26.
- 9 R. J. Gryglewski, R. M. J. Palmer and S. Moncada, *Nature*, 1986, **320**, 454–456.
- 10 T. B. McCall, N. K. Boughton-Smith, R. M. J. Palmer, B. J. R. Whittle and S. Moncada, *Biochem. J.*, 1989, **261**, 293–296.
- 11 Y. Xia, V. L. Dawson, T. M. Dawson, S. H. Snyder and J. L. Zweier, *Proc. Natl. Acad. Sci. U. S. A.*, 1996, **93**, 6770–6774.
- 12 J. S. Beckman, T. W. Beckman, J. Chen, P. A. Marshall and B. A. Freeman, *Proc. Natl. Acad. Sci. U. S. A.*, 1990, **87**, 1620–1624.
- 13 P. Pacher, J. S. Beckman and L. Liaudet, *Physiol. Rev.*, 2007, **87**, 315–424.
- 14 R. Kissner, T. Nauser, P. Bugnon, P. G. Lye and W. H. Koppenol, *Chem. Res. Toxicol.*, 1997, **10**, 1285–1292.
- 15 M. Anbar and H. Taube, *J. Am. Chem. Soc.*, 1954, **76**, 6243–6247.
- 16 J. D. Ray, *J. Inorg. Nucl. Chem.*, 1962, **24**, 1159–1162.
- 17 W. H. Koppenol, J. J. Moreno, W. A. Pryor, H. Ischiropoulos and J. S. Beckman, *Chem. Res. Toxicol.*, 1992, **5**, 834–842.
- 18 C. Kurz, X. Zeng, S. Hannemann, R. Kissner and W. H. Koppenol, *J. Phys. Chem. A*, 2005, **109**, 965–969.
- 19 W. H. Koppenol, P. L. Bounds, T. Nauser, R. Kissner and H. Ruegger, *Dalton Trans.*, 2012, **41**, 13779–13787.
- 20 W. G. Keith and R. E. Powell, *J. Chem. Soc. A*, 1969, 90–90.
- 21 S. V. Lyman and J. K. Hurst, *J. Am. Chem. Soc.*, 1995, **117**, 8867–8868.
- 22 A. Denicola, B. A. Freeman, M. Trujillo and R. Radi, *Arch. Biochem. Biophys.*, 1996, **333**, 49–58.
- 23 D. M. Stanbury, *Adv. Inorg. Chem.*, 1989, **33**, 69–138.
- 24 R. E. Huie, C. L. Clifton and P. Neta, *Radiat. Phys. Chem.*, 1991, **38**, 477–481.
- 25 S. V. Lyman, Q. Jiang and J. K. Hurst, *Biochemistry*, 1996, **35**, 7855–7861.
- 26 M. S. Ramezanian, S. Padmaja and W. H. Koppenol, *Chem. Res. Toxicol.*, 1996, **9**, 232–240.
- 27 J. N. Lemercier, S. Padmaja, R. Cueto, G. L. Squadrato, R. M. Uppu and W. A. Pryor, *Arch. Biochem. Biophys.*, 1997, **345**, 160–170.
- 28 F. Barat, L. Gilles, B. Hickel and J. Sutton, *J. Chem. Soc. A*, 1970, 1982–1986.
- 29 T. Løgager and K. Sehested, *J. Phys. Chem.*, 1993, **97**, 6664–6669.
- 30 B. Alvarez and R. Radi, First Int. Conf. Chemistry and Biology of Peroxynitrite, Ascona, 1997, 2–2.
- 31 W. H. Koppenol and R. Kissner, *Chem. Res. Toxicol.*, 1998, **11**, 87–90.

- 32 P. Maurer, C. F. Thomas, R. Kissner, H. Rüegger, O. Greter, U. Röthlisberger and W. H. Koppenol, *J. Phys. Chem. A*, 2003, **107**, 1763–1769.
- 33 J. S. Beckman, H. Ischiropoulos, L. Zhu, M. van der Woerd, C. D. Smith, J. Chen, J. Harrison, J. C. Martin and M. Tsai, *Arch. Biochem. Biophys.*, 1992, **298**, 438–445.
- 34 R. Radi, J. S. Beckman, K. M. Bush and B. A. Freeman, *Arch. Biochem. Biophys.*, 1991, **288**, 481–487.
- 35 S. Pfeiffer, A. C. F. Gorren, K. Schmidt, E. R. Werner, B. Hansert, D. S. Bohle and B. Mayer, *J. Biol. Chem.*, 1997, **272**, 3465–3470.
- 36 R. Kissner and W. H. Koppenol, *J. Am. Chem. Soc.*, 2002, **124**, 234–239.
- 37 M. Kirsch, H.-G. Korth, A. Wensing, R. Sustmann and H. de Groot, *Arch. Biochem. Biophys.*, 2003, **418**, 133–150.
- 38 D. Gupta, B. Harish, R. Kissner and W. H. Koppenol, *Dalton Trans.*, 2009, 5730–5736.
- 39 T. Løgager and K. Sehested, *J. Phys. Chem.*, 1993, **97**, 10047–10052.
- 40 S. Goldstein and G. Czapski, *Inorg. Chem.*, 1997, **36**, 4156–4162.
- 41 D. S. Bohle, B. Hansert, S. C. Paulson and B. D. Smith, *J. Am. Chem. Soc.*, 1994, **116**, 7423–7424.
- 42 S. Miyamoto, G. E. Ronsein, T. C. Corrêa, G. R. Martinez, M. H. G. Medeiros and P. Di Mascio, *Dalton Trans.*, 2009, 5720–5729.
- 43 S. Goldstein, G. Czapski, J. Lind and G. Merényi, *Inorg. Chem.*, 1998, **37**, 3943–3947.
- 44 W. H. Koppenol, *Inorg. Chem.*, 2012, **51**, 5637–5641.
- 45 W. H. Koppenol, D. M. Stanbury and P. L. Bounds, *Free Radical Biol. Med.*, 2010, **49**, 317–322.
- 46 D. D. Wagman, W. H. Evans, V. B. Parker, R. H. Schumm, I. Halow, S. M. Bailey, K. L. Churney and R. L. Nuttal, *J. Phys. Chem. Ref. Data*, 1982, **11**(Suppl. 2), 37–38.
- 47 P. Warneck and C. Wurzinger, *J. Phys. Chem.*, 1988, **92**, 6278–6283.
- 48 M. Kirsch, E. E. Lomonosova, H.-G. Korth, R. Sustmann and H. de Groot, *J. Biol. Chem.*, 1998, **273**, 12716–12724.
- 49 S. Kapiotis, M. Hermann, I. Held, A. Mühl and B. Gmeiner, *FEBS Lett.*, 1997, **409**, 223–226.
- 50 D. Tsikas, K. Denker and J. C. Fröhlich, *J. Chromatogr. A*, 2001, **915**, 107–116.
- 51 E. Pollet, J. A. Martínez, B. Metha, B. P. Watts Jr. and J. F. Turrens, *Arch. Biochem. Biophys.*, 1998, **349**, 74–80.
- 52 D. S. Bohle, P. A. Glassbrenner and B. Hansert, *Methods Enzymol.*, 1996, **269**, 302–311.
- 53 P. Latal, R. Kissner, D. S. Bohle and W. H. Koppenol, *Inorg. Chem.*, 2004, **43**, 6519–6521.
- 54 R. M. Smith and A. E. Martell, *Critical Stability Constants: Volume 4: Inorganic Complexes*, 1976.
- 55 R. Kissner, T. Nauser, C. Kurz and W. H. Koppenol, *IUBMB Life*, 2003, **55**, 567–572.
- 56 D. F. Evans and M. W. Upton, *J. Chem. Soc., Dalton Trans.*, 1985, 1151–1153.
- 57 J. F. Goodman, P. Robson and E. R. Wilson, *Trans. Faraday Soc.*, 1962, **58**, 1846–1851.
- 58 E. Koubek, M. L. Haggett, C. J. Bataglia, K. M. Ibne-Rasa, H. Y. Pyun and J. O. Edwards, *J. Am. Chem. Soc.*, 1963, **85**, 2263–2268.
- 59 Z. Yuan, Y. Ni and A. R. P. van Heiningen, *Can. J. Chem. Eng.*, 1997, **75**, 37–41.